High Temperature Superconductivity in a Lightly Doped Quantum Spin Liquid

Hong-Chen Jiang [1,*] and Steven A. Kivelson [2]

[1] Stanford Institute for Materials and Energy Sciences, SLAC National Accelerator Laboratory and Stanford University, Menlo Park, California 94025, USA

[2] Department of Physics, Stanford University, Stanford, California 94305, USA

(Received 4 April 2021; accepted 20 July 2021; published 27 August 2021)

We have performed density-matrix renormalization group studies of a square lattice t-J model with small hole doping, $\delta \ll 1$, on long four and six-leg cylinders. We include frustration in the form of a second-neighbor exchange coupling, $J_2 = J_1/2$, such that the undoped ($\delta = 0$) "parent" state is a quantum spin liquid. In contrast to the relatively short range superconducting (SC) correlations that have been observed in recent studies of the six-leg cylinder in the absence of frustration, we find power-law SC correlations with a Luttinger exponent, $K_{\mathrm{SC}} \approx 1$, consistent with a strongly diverging SC susceptibility, $\chi \sim T^{-(2-K_{\mathrm{SC}})}$ as the temperature $T \to 0$. The spin-spin correlations—as in the undoped state—fall exponentially suggesting that the SC "pairing" correlations evolve smoothly from the insulating parent state.

DOI: 10.1103/PhysRevLett.127.097002

Although the physics of cuprate high temperature superconductors is surely complex, there are a variety of reasons [1–3] to believe that the "essential" [4] physics is captured by the two-dimensional (2D) Hubbard model or its close relatives. To begin with, as is the case in cuprates, in an appropriate regime of parameters, the Hubbard model on a square lattice with $n = 1$ electrons per site exhibits an undoped "parent" state that is a Mott insulating antiferromagnet. However, two key theoretical issues concerning this proposition remain unsettled: (1) Does d-wave superconductivity (SC) "robustly" arise in this model upon light doping, i.e., for $0 < \delta \equiv (1 - n) \ll 1$? (2) If so, how does it arise (i.e., what is the "mechanism") and under what circumstances (e.g., does it depend on specific features of the band structure)?

For parametrically small values of the Hubbard $U \ll W$ (where W is the bandwidth), it is possible to establish [5] that such a superconducting state arises, but here (except under extremely fine-tuned circumstances in which the Fermi surface is perfectly nested) the undoped state at $n = 1$ is also superconducting, and the superconducting T_c is exponentially small in units of W. For intermediate $U \sim W$, no controlled analytic approach exists, but calculations based on a variety of physically motivated approximations [6–8] yield results suggestive of values of T_c as large as $T_c \sim W$ [where the proportionality is a number of order 1 but may be small, e.g., $\sim(2\pi)^{-2}$]. This was further supported by density-matrix normalization group (DMRG) studies of the Hubbard and t-J models on four-leg square cylinders [9–13]. However, recent [14] DMRG calculations on six-leg square cylinders, as well as variational Monte Carlo [15] calculations on 2D models, have called this proposition into question. Specifically, the tendency of a doped antiferromagnet to phase separation [15,16] or to charge-density wave (CDW) formation [11,13,14,17–21] appears to play a much more dominant role in the physics at small δ than accounted for by most approximate approaches.

One attractive notion that was suggested early on is that high temperature superconductivity could arise naturally [1,22–27] under circumstances in which the insulating parent state is a quantum spin liquid (QSL) rather than an ordered antiferromagnet. In particular, a QSL with a gap (even a partial gap with nodes), can in some sense be thought of as a state with preexisting Cooper pairs but with vanishing superfluid stiffness. Then, upon light doping, one might naturally expect SC with a gap scale that is inherited from the QSL (i.e., evolves continuously as $\delta \to 0$) and with a superfluid stiffness—that rises with δ.

In the present Letter, we explore the possibility of SC in a doped spin liquid using DMRG to treat the t-J model (a proxy for the Hubbard model) on cylinders of circumference 4 and 6. A number of studies of the spin-1/2 Heisenberg model on the square lattice with first and second neighbor exchange couplings, J_1 and J_2, have led to a consensus [28–35] that there is a QSL phase in the range of $0.46 < J_2/J_1 < 0.52$ [35]. In this range, DMRG on cylinders of circumference up to $L_y = 10$ show a pronounced spin-gap and exponentially falling spin-spin correlations with a correlation length ξ_s considerably smaller than L_y [30,32]. However, there is still some debate about whether this gap persists in the 2D limit, or if instead the QSL phase has a gapless nodal spinon spectrum.

Here, we study the model with $J_2/J_1 = 0.5$, and correspondingly we take the ratio of nearest to next-nearest neighbor hopping matrix elements, $t_2/t_1 = 0.7 \approx \sqrt{J_2/J_1}$, and a value of $J_1/t_1 = 1/3$ corresponding loosely to a value of $U \approx 4t^2/J = 12t$. On the cylinders we study, the undoped system is fully gapped, so it effectively corresponds to a compactified version of a gapped Z_2 spin liquid of the sort that arises in the quantum dimer model [36,37] and the toric code model [38]. Upon lightly doping we find a state which still shows exponentially falling spin-spin correlations, with correlation lengths that are longer than but of the same order as in the undoped system. Most importantly, we find that even at the smallest δ and on our largest six-leg cylinders, the SC correlations are strong and decay with a slow power law, $\sim |r|^{-K_{\mathrm{SC}}}$, with $K_{\mathrm{SC}} \approx 1$. This slow decay implies a SC susceptibility that diverges as $\chi_{\mathrm{SC}} \sim T^{-(2-K_{\mathrm{SC}})}$ as $T \to 0$. As far as we know, to date, this is the strongest indication of SC that has been found in any DMRG study of a system on the square lattice of width $L_y > 4$. Moreover, the SC correlations dominate over the CDW correlations in the sense that in all cases $K_c > K_{\mathrm{SC}}$. This is suggestive that SC order is realized in the 2D limit, although given that in all cases the CDW correlations are substantial, this inference remains speculative.

Model and method.—We employ DMRG [39] to study the ground state properties of the hole-doped *t-J* model on the square lattice, which is defined by the Hamiltonian

$$H = -\sum_{ij\sigma} t_{ij}(\hat{c}^\dagger_{i\sigma}\hat{c}_{j\sigma} + \mathrm{H.c.}) + \sum_{ij} J_{ij}\left(\vec{S}_i \cdot \vec{S}_j - \frac{\hat{n}_i \hat{n}_j}{4}\right).$$

Here $\hat{c}^\dagger_{i\sigma}$ ($\hat{c}_{i\sigma}$) is the electron creation (annihilation) operator on site $i = (x_i, y_i)$ with spin polarization σ, $\vec{S}_i$ is the spin operator, and $\hat{n}_i = \sum_\sigma \hat{c}^\dagger_{i\sigma}\hat{c}_{i\sigma}$ is the electron number operator. The electron hopping amplitude t_{ij} is equal to t_1 (t_2) if i and j are nearest neighbor (NN) and (NNN) sites. J_1 and J_2 are the spin superexchange interactions between NN and NNN sites, respectively. The Hilbert space is constrained by the no-double occupancy condition, $n_i \leq 1$. At half-filling, i.e., $n_i = 1$, H reduces to the spin-1/2 antiferromagnetic J_1-J_2 Heisenberg model.

We take the lattice geometry to be cylindrical with periodic and open boundary conditions in the $\hat{y}$ and $\hat{x}$ directions, respectively. Here $\hat{y} = (0,1)$ and $\hat{x} = (1,0)$ are the two basis vectors of the square lattice. Here, we focus on cylinders with width L_y and length L_x, where L_x and L_y are the number of sites along the $\hat{x}$ and $\hat{y}$ directions, respectively. The total number of sites is $N = L_x \times L_y$, the number of electrons N_e, and the doping level of the system is defined as $\delta = N_h/N$, where $N_h = N - N_e$ is the number of doped holes relative to the half-filled insulator with $N_e = N$. In the present study, we focus on $L_y = 4$ cylinders of length up to $L_x = 128$ and $L_y = 6$ cylinders of length up to $L_x = 48$, and for values of $\delta = 1/18$, $1/16$, and $1/12$. We set $J_1 = 1$ as an energy unit and $J_2 = 0.5$ such that the undoped system is deep in the QSL phase at half-filling [28,30,32,35]. We consider $t_1 = 3$ and $t_2 = t_1\sqrt{J_2/J_1}$ to make a connection to the corresponding Hubbard model. We perform up to 90 sweeps and keep up to $m = 10\,000$ states for $L_y = 4$ cylinders with a typical truncation error $\epsilon < 10^{-7}$, and up to $m = 40\,000$ states for $L_y = 6$ cylinders with a typical truncation error $\epsilon < 10^{-6}$. Further details of the numerical simulation are provided in the Supplemental Material (SM) [40].

Superconducting pair-field correlations.—We have calculated the equal-time spin-singlet SC pair-field correlation function

$$\Phi_{\alpha\beta}(r) = \frac{1}{L_y}\sum_{y=1}^{L_y} |\langle \Delta^\dagger_\alpha(x_0, y)\Delta_\beta(x_0 + r, y)\rangle|. \qquad (1)$$

$\Delta^\dagger_\alpha(x,y) = (1/\sqrt{2})[\hat{c}^\dagger_{(x,y),\uparrow}\hat{c}^\dagger_{(x,y)+\alpha,\downarrow} + \hat{c}^\dagger_{(x,y)+\alpha,\uparrow}\hat{c}^\dagger_{(x,y),\downarrow}]$ is the spin-singlet pair creation operator on bond $\alpha = \hat{x}$ or $\hat{y}$, where (x_0, y) is a reference bond taken as $x_0 \sim L_x/4$ and r is the displacement between bonds in the $\hat{x}$ direction.

Figure 1 shows $\Phi_{yy}(r)$ for both $L_y = 4$ and $L_y = 6$ cylinders at different doping levels. At long distance, $\Phi(r)$ is characterized by a power law with the appropriate Luttinger exponent K_{SC} defined by

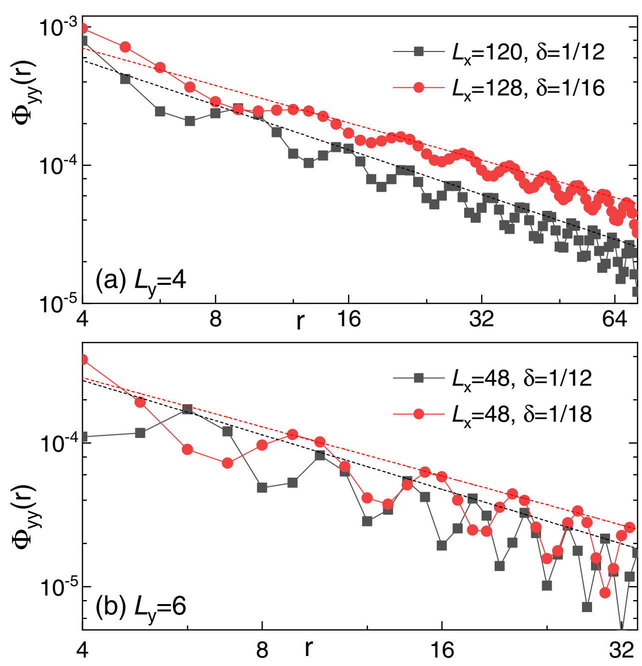

FIG. 1. Superconducting pair-field correlations $\Phi_{yy}(r)$ on double-logarithmic scales for (a) $L_y = 4$ cylinders at $\delta = 1/12$ and $\delta = 1/16$, and (b) $L_y = 6$ cylinders at $\delta = 1/12$ and $\delta = 1/18$. r is the distance between two Cooper pairs in the $\hat{x}$ direction. The dashed lines denote power-law fitting to $\Phi_{yy}(r) \sim r^{-K_{\mathrm{SC}}}$.

$$\Phi(r) \sim r^{-K_{\rm SC}}. \qquad (2)$$

The exponent $K_{\rm SC}$, which is obtained by fitting the results using Eq. (2), is $K_{\rm SC} = 1.08(4)$ for $\delta = 1/12$ and $K_{\rm SC} = 0.95(2)$ for $\delta = 1/16$ on $L_y = 4$ cylinders, and $K_{\rm SC} = 1.26(7)$ for $\delta = 1/12$ and $K_{\rm SC} = 1.14(5)$ for $\delta = 1/18$ on $L_y = 6$ cylinders. This establishes that the lightly doped QSL on both $L_y = 4$ and $L_y = 6$ cylinders has quasi-long-range SC correlations. In addition to $\Phi_{yy}(r)$, we have also calculated components of the tensor—$\Phi_{xx}(r)$ and $\Phi_{xy}(r)$—and find that $\Phi_{xx}(r) \sim \Phi_{yy}(r) \sim -\Phi_{xy}(r)$. In short, the SC correlations have a d-wave form.

CDW correlations.—To measure the charge order, we define the rung density operator $\hat{n}(x) = L_y^{-1} \sum_{y=1}^{L_y} \hat{n}(x, y)$ and its expectation value $n(x) = \langle \hat{n}(x) \rangle$. Figure 2(a) shows the charge density distribution $n(x)$ for $L_y = 4$ cylinders, which is consistent with "half-filled charge stripes" with wavelength $\lambda = 1/2\delta$. This corresponds to an ordering wave vector $Q = 4\pi\delta$ corresponding to half a doped hole per 2D unit cell, i.e., viewing the cylinder as a 1D system, two holes per 1D unit cell. The charge density profile $n(x)$ for $L_y = 6$ cylinders is shown in Fig. 2(b), which has wavelength $\lambda = 1/3\delta$, consistent with "third-filled" charge stripes. This corresponds to an ordering wave vector $Q = 6\pi\delta$ and one third of a doped hole per 2D unit cell—again corresponding to two holes per 1D unit cell.

At long distance, the spatial decay of the CDW correlation is dominated by a power law with the Luttinger exponent K_c. The exponent K_c can be obtained by fitting the charge density oscillations (Friedel oscillations) induced by the boundaries of the cylinder [43]

$$n(x) = n_0 + A_Q * \cos(Qx + \phi) x^{-K_c/2}. \qquad (3)$$

Here A_Q is an amplitude, ϕ is a phase shift, $n_0 = 1 - \delta$ is the mean density, and $Q = 4\pi\delta$. Note that a few data points [Figs. 2(a) and 2(b), light grey color] are excluded to minimize the boundary effect and improve the fitting quality. The extracted exponents for $L_y = 4$ cylinders are $K_c = 1.29(3)$ when $\delta = 1/12$ and $K_c = 1.37(3)$ when $\delta = 1/16$. For $L_y = 6$ cylinders, $K_c = 1.42(5)$ when $\delta = 1/12$ and $K_c = 1.55(5)$ when $\delta = 1/18$. Similarly, K_c can also be obtained from the charge density-density fluctuation correlation which gives qualitatively consistent results (see SM).

Spin-spin correlations.—To describe the magnetic properties of the ground state, we calculate the spin-spin correlation functions defined as

$$F(r) = \frac{1}{L_y} \sum_{y=1}^{L_y} |\langle \vec{S}_{x_0,y} \cdot \vec{S}_{x_0+r,y} \rangle|. \qquad (4)$$

Figure 3 shows $F(r)$ for $L_y = 6$ cylinders at different doping levels, which decays exponentially as $F(r) \sim e^{-r/\xi_s}$ at long distances, with a correlation length $\xi_s = 3.98(1)$ lattice spacings for $\delta = 1/12$ and $\xi_s = 3.06(2)$ lattice spacings for $\delta = 1/18$. For comparison, the spin-spin correlation $F(r)$ at half-filling, i.e., $\delta = 0$, is also shown, which decays exponentially with a correlation length $\xi_s = 1.42(1)$. Therefore, the spin-spin correlations at finite doping levels are short ranged and similar to those of the QSL at half-filling. In the inset of Fig. 3, we show the spin

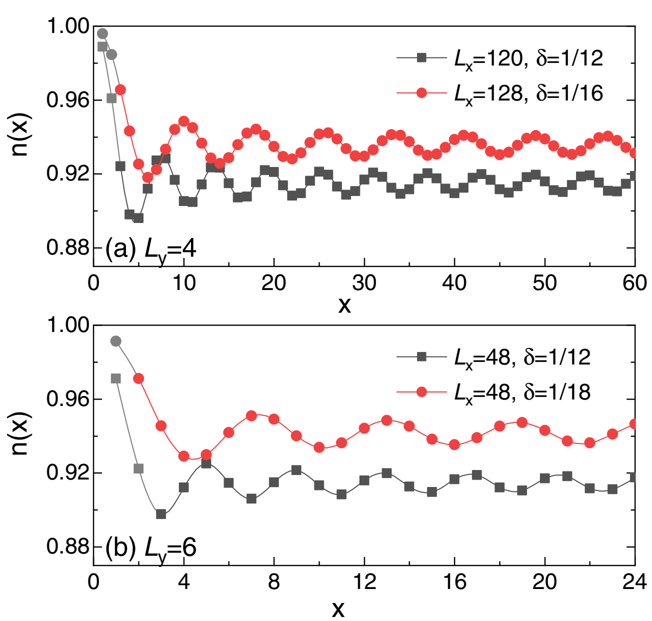

FIG. 2. Charge density profiles $n(x)$ for (a) $L_y = 4$ cylinders at $\delta = 1/12$ and $\delta = 1/16$, and (b) $L_y = 6$ cylinders at $\delta = 1/12$ and $\delta = 1/18$. The exponent K_c is extracted using Eq. (3), with the data points in grey neglected to minimize boundary effects.

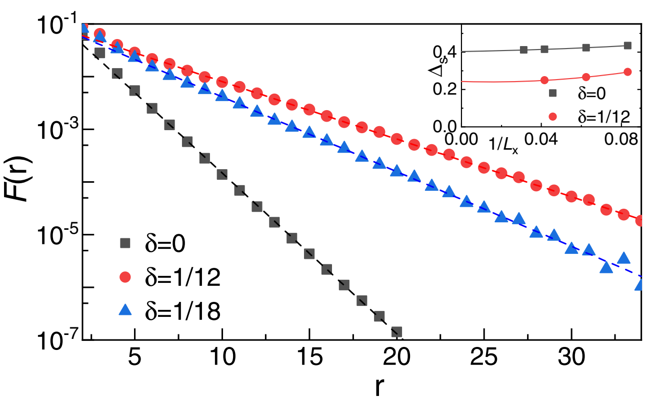

FIG. 3. Spin-spin correlations $F(r)$ for $L_y = 6$ cylinders at $\delta = 0$, $\delta = 1/12$ and $\delta = 1/18$ on the semilogarithmic scale. Dashed lines denote exponential fit $F(r) \sim e^{-r/\xi_s}$, where r is the distance between two sites in the $\hat{x}$ direction. Inset: spin gap Δ_s for $L_y = 6$ cylinders at $\delta = 0$ and $\delta = 1/12$. Solid lines denote second-order polynomial fitting.

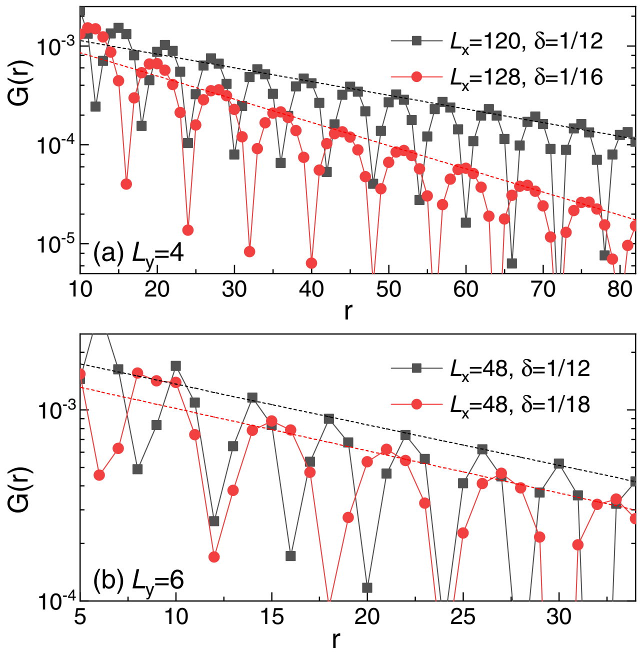

FIG. 4. Single-particle Green function $G(r)$ for (a) $L_y = 4$ cylinders at $\delta = 1/12$ and $\delta = 1/16$, and (b) $L_y = 6$ cylinders at $\delta = 1/12$ and $\delta = 1/18$ on the semilogarithmic scale. Dashed line denote exponential fitting $G(r) \sim e^{-r/\xi_G}$ where r is the distance between two sites in the $\hat{x}$ direction.

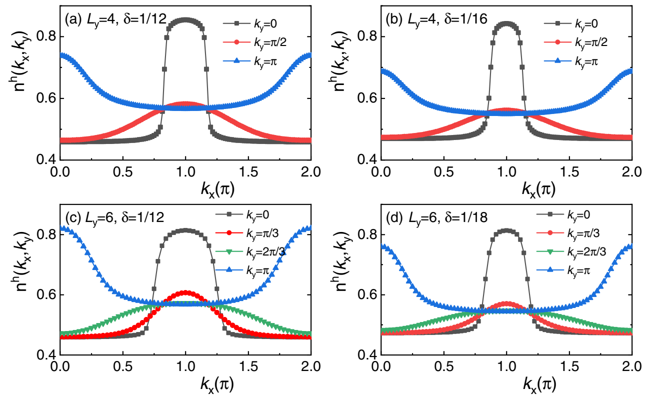

FIG. 5. Hole momentum distribution function $n^h(k_x, k_y)$ for $L_y = 4$ cylinders at (a) $\delta = 1/12$ and (b) $\delta = 1/16$, and $L_y = 6$ cylinders at (c) $\delta = 1/12$ and (d) $\delta = 1/18$ at different k_y as a function of k_x in unit of π.

gap, defined as $\Delta_s = E_0(S_z = 1) - E_0(S_z = 0)$, where $E_0(S_z)$ is the ground state energy of a system with total spin S_z. At half-filling, i.e., $\delta = 0$, $\Delta_s = 0.40(1)$ which is consistent with previous studies [30,32]. At $\delta = 1/12$, $\Delta_s = 0.24(1)$, which is consistent with the short-range nature of $F(r)$.

Single particle Green function.—We have also calculated the single-particle Green function, defined as

$$G(r) = \frac{1}{L_y} \sum_{y=1}^{L_y} \langle c^\dagger_{(x_0,y),\sigma} c_{(x_0+r,y),\sigma} \rangle. \tag{5}$$

Figure 4 shows $G(r)$ for both $L_y = 4$ and $L_y = 6$ cylinders at different doping levels, the long distance behavior of G is consistent with exponential decay $G(r) \sim e^{-r/\xi_G}$. The extracted correlation lengths for $L_y = 4$ cylinders are $\xi_G = 30(2)$ when $\delta = 1/12$ and $\xi_G = 18(1)$ when $\delta = 1/16$, while for $L_y = 6$ cylinders, $\xi_G = 21(1)$ when $\delta = 1/12$ and $\xi_G = 20(2)$ when $\delta = 1/18$.

We have also measured the hole momentum distribution function defined as

$$n^h(\mathbf{k}) = \frac{1}{2}\left[2 - \sum_\sigma n_\sigma(\mathbf{k})\right]. \tag{6}$$

Here $n_\sigma(\mathbf{k}) = (1/N)\sum_{ij} e^{i\mathbf{k}\cdot(\mathbf{r}_i - \mathbf{r}_j)} \langle \hat{c}^\dagger_{i\sigma} \hat{c}_{j\sigma} \rangle$ is the electron momentum distribution function for an electron with spin-σ. Figure 5 shows $n^h(\mathbf{k})$ for both $L_y = 4$ and $L_y = 6$ cylinders at different doping levels. Not surprisingly, there are no clear discontinuities in $n^h(\mathbf{k})$ of the sort that would be expected at the Fermi momenta of a Fermi liquid.

However, there are sharp drops in $n^h(\mathbf{k})$ (which can be identified as maxima of $|dn^h(\mathbf{k})/dk_x|$) (see SM for details) that are suggestive of the "near existence" of a Fermi surface. These features are most prominent for $k_y = 0$, where they occur at $k_x \approx \pi \pm k_0$, but there are slightly broader features of the same general sort for $k_y = \pi$, at $k_x = \pm k_\pi$. For $L_y = 4$ and $\delta = 1/16$, $k_0 = 0.075\pi$ and $k_\pi = 0.175\pi$; for $L_y = 4$ and $\delta = 1/12$, $k_0 = 0.175\pi$ and $k_\pi = 0.192\pi$; for $L_y = 6$ and $\delta = 1/18$, $k_0 = 0.17\pi$ and $k_\pi = 0.18\pi$; for $L_y = 6$ and $\delta = 1/12$, $k_0 = 0.25\pi$ and $k_\pi = 0.25\pi$. Within the numerical uncertainty, there is a direct relation between these quasi-Fermi momenta and the CDW ordering vector: $Q = 2(k_0 + k_\pi)$. Moreover, since $Q = \pi L_y \delta$, this corresponds to the expected value of $2k_F$ that would correspond to the "volume" of the Fermi surface under conditions (not satisfied in the present case) in which Luttinger's theorem applies.

Conclusion.—There is necessarily a speculative leap from results on finite cylinders to the 2D limit. However, we feel that the present results—and those of a similar study by one of us on the triangular lattice t-J model on four- and six-leg cylinders [44,45]—can plausibly be taken as representative of the solution of the corresponding 2D problem. In particular, they support the proposition that SC can emerge upon light doping of a QSL [46].

Conversely, our earlier observation of an insulating holon crystal in a lightly doped Kagome system [47,48] and CDW order in a lightly doped honeycomb Kiatev spin liquid [49] imply that SC is not the universal result of doping a QSL. Indeed, for otherwise identical cylinders to those reported above, reversing the sign of t_2 (i.e., taking

$t_2 = -t_1\sqrt{J_2/J_1}$) reduces the long distance SC correlations by many orders of magnitude although whether some weak SC power-law correlations persist is still unsettled. Moreover, we have also found greatly enhanced SC correlations on four- and six-leg cylinders with a spatially modulated ("striped") version of the square-lattice Hubbard model [50]; it thus may be aspects of doping a quantum paramagnet (i.e., a system in which quantum fluctuations are sufficient to destroy magnetic order) rather than specific features of a doped QSL that are responsible for the strong SC tendencies.

It is harder still to make inferences about T_c itself in the 2D limit. The large values of the spin gaps, $\Delta_s \sim J/4$, are suggestive that pairing is sufficiently strong to persist to very high T. It is therefore likely that T_c is determined by the phase ordering scale [51], in other words that the zero temperature superfluid stiffness and hence T_c itself rise roughly linearly with δ for $\delta \ll 1$ [22].

We would like to thank Erez Berg, Johannes Motruk, Zheng-Yu Weng, and Yi-Fan Jiang for helpful discussions. This work was supported by the Department of Energy, Office of Science, Basic Energy Sciences, Materials Sciences and Engineering Division, under Contract DE-AC02-76SF00515.

Note added.—We have become aware of two independent but closely related DMRG studies of the t-t'-J model by Gong, Zhu, and Sheng [52] (GZS) and Jiang, Scalapino, and White [53] (JSW). Both report results for six-leg cylinders, while JSW also have results for eight-leg cylinders. Both studies investigated t' in the range $0 \le t' \le 0.3t$—i.e., neither include the large value $t' = t/\sqrt{2}$ studied here. JSW also studied negative t'—the sign that is thought to be relevant to the hole-doped cuprates—in the range $-0.3t \le t \le 0$. Overall, the two papers agree that increasing (positive) t' tends to increase the tendency to d-wave SC order and decrease the tendency to various sorts of competing SDW and CDW orders, which also correlates well with our observations at larger t'. Conversely, JSW find that negative t' strengthens stripe order and depresses SC order, consistent with our already mentioned failure to find strong SC tendencies for $t' = -t/\sqrt{2}$. One should notice, however, that there are significant differences in other aspects of the inferred phase diagrams reported by GZS and JSW—which likely reflects the delicate nature of the phase competition between multiple phases that occurs in the range of t' and doping they have explored.

*hcjiang@stanford.edu

[1] P. W. Anderson, The Resonating valence bond state in La_2CuO_4 and superconductivity, Science **235**, 1196 (1987).
[2] V. J. Emery, Theory of High-T_c Superconductivity in Oxides, Phys. Rev. Lett. **58**, 2794 (1987).
[3] D. J. Scalapino, A common thread: The pairing interaction for unconventional superconductors, Rev. Mod. Phys. **84**, 1383 (2012).
[4] S. Kivelson and S. Kivelson, Understanding complexity, Nat. Phys. **14**, 426 (2018).
[5] S. Raghu, S. A. Kivelson, and D. J. Scalapino, Superconductivity in the repulsive Hubbard model: An asymptotically exact weak-coupling solution, Phys. Rev. B **81**, 224505 (2010).
[6] E. Gull and A. J. Millis, Quasiparticle properties of the superconducting state of the two-dimensional Hubbard model, Phys. Rev. B **91**, 085116 (2015).
[7] P. Staar, M. Jiang, U. R. Hähner, T. C. Schulthess, and T. A. Maier, Interlaced coarse-graining for the dynamic cluster approximation, Phys. Rev. B **93**, 165144 (2016).
[8] Y. Wang, A. Abanov, B. L. Altshuler, E. A. Yuzbashyan, and A. V. Chubukov, Superconductivity near a Quantum-Critical Point: The Special Role of the First Matsubara Frequency, Phys. Rev. Lett. **117**, 157001 (2016).
[9] H.-C. Jiang, Z.-Y. Weng, and S. A. Kivelson, Superconductivity in the doped $t-J$ model: Results for four-leg cylinders, Phys. Rev. B **98**, 140505(R) (2018).
[10] H.-C. Jiang and T. P. Devereaux, Superconductivity in the doped hubbard model and its interplay with next-nearest hopping t', Science **365**, 1424 (2019).
[11] Y.-F. Jiang, J. Zaanen, T. P. Devereaux, and H.-C. Jiang, Ground state phase diagram of the doped hubbard model on the four-leg cylinder, Phys. Rev. Research **2**, 033073 (2020).
[12] H.-C. Jiang, S. Chen, and Z.-Y. Weng, Critical role of the sign structure in the doped mott insulator: Luther-emery versus fermi-liquid-like state in quasi-one-dimensional ladders, Phys. Rev. B **102**, 104512 (2020).
[13] C.-M. Chung, M. Qin, S. Zhang, U. Schollwöck, and S. R. White, Plaquette versus ordinary d-wave pairing in the t'-hubbard model on a width-4 cylinder, Phys. Rev. B **102**, 041106(R) (2020).
[14] J. P. F. LeBlanc *et al.*, Solutions of the Two-Dimensional Hubbard Model: Benchmarks and Results from a Wide Range of Numerical Algorithms, Phys. Rev. X **5**, 041041 (2015).
[15] S. Sorella, The phase diagram of the Hubbard model by variational auxiliary field quantum Monte Carlo, arXiv:2101.07045.
[16] V. J. Emery, H. Q. Lin, and S. A. Kivelson, Phase Separation in the $t-J$ Model, Phys. Rev. Lett. **64**, 475 (1990).
[17] J. Zaanen and O. Gunnarsson, Charged magnetic domain lines and the magnetism of high-T_c oxides, Phys. Rev. B **40**, 7391 (1989).
[18] H. J. Schulz, Domain walls in a doped antiferromagnet, J. Phys. France **50**, 2833 (1989).
[19] K. Machida, Magnetism in La_2CuO_4 based compounds, Physica (Amsterdam) **158C**, 192 (1989).
[20] S. R. White and D. J. Scalapino, Ground states of the doped four-leg t-J ladder, Phys. Rev. B **55**, R14701 (1997).
[21] M. Qin, C.-M. Chung, H. Shi, E. Vitali, C. Hubig, U. Schollwöck, S. R. White, and S. Zhang, Absence of

Superconductivity in the Pure Two-Dimensional Hubbard Model, Phys. Rev. X **10**, 031016 (2020).
[22] S. A. Kivelson, D. S. Rokhsar, and J. P. Sethna, Topology of the resonating valence-bond state–solitons and High T_c superconductivity, Phys. Rev. B **35**, 8865 (1987).
[23] R. B. Laughlin, The relationship between high-temperature superconductivity and the fractional quantum Hall effect, Science **242**, 525 (1988).
[24] G. Kotliar, Resonating valence bonds and d-wave superconductivity, Phys. Rev. B **37**, 3664 (1988).
[25] L. Balents, M. P. A. Fisher, and C. Nayak, Nodal liquid theory of the pseudo-gap phase of high-T_c superconductors, Int. J. Mod. Phys. B **12**, 1033 (1998).
[26] P. W. Anderson, P. A. Lee, M. Randeria, T. M. Rice, N. Trivedi, and F. C. Zhang, The physics behind high-temperature superconducting cuprates: The 'plain vanilla' version of RVB, J. Phys. Condens. Matter **16**, R755 (2004).
[27] X.-Y. Song, A. Vishwanath, and Y.-H. Zhang, Doping the chiral spin liquid–topological superconductor or chiral metal? Phys. Rev. B **103**, 165138 (2021).
[28] F. Figueirido, A. Karlhede, S. Kivelson, S. Sondhi, M. Rocek, and D. S. Rokhsar, Exact diagonalization of finite frustrated spin-$\frac{1}{2}$ Heisenberg models, Phys. Rev. B **41**, 4619 (1990).
[29] L. Capriotti, F. Becca, A. Parola, and S. Sorella, Resonating Valence Bond Wave Functions for Strongly Frustrated Spin Systems, Phys. Rev. Lett. **87**, 097201 (2001).
[30] H.-C. Jiang, H. Yao, and L. Balents, Spin liquid ground state of the spin-$\frac{1}{2}$ square J_1-J_2 heisenberg model, Phys. Rev. B **86**, 024424 (2012).
[31] W.-J. Hu, F. Becca, A. Parola, and S. Sorella, Direct evidence for a gapless Z_2 spin liquid by frustrating néel antiferromagnetism, Phys. Rev. B **88**, 060402(R) (2013).
[32] S.-S. Gong, W. Zhu, D. N. Sheng, O. I. Motrunich, and M. P. A. Fisher, Plaquette Ordered Phase and Quantum Phase Diagram in the Spin-$\frac{1}{2}$ J_1-J_2 Square Heisenberg Model, Phys. Rev. Lett. **113**, 027201 (2014).
[33] S. Morita, R. Kaneko, and M. Imada, Quantum spin liquid in spin $1/2$ $j_1 - j_2$ heisenberg model on square lattice: Many-variable variational monte carlo study combined with quantum-number projections, J. Phys. Soc. Jpn. **84**, 024720 (2015).
[34] L. Wang, Z.-C. Gu, F. Verstraete, and X.-G. Wen, Tensor-product state approach to spin-$\frac{1}{2}$ square $J_1 - J_2$ antiferromagnetic heisenberg model: Evidence for deconfined quantum criticality, Phys. Rev. B **94**, 075143 (2016).
[35] L. Wang and A. W. Sandvik, Critical Level Crossings and Gapless Spin Liquid in the Square-Lattice Spin-$1/2$ $J_1 - J_2$ Heisenberg Antiferromagnet, Phys. Rev. Lett. **121**, 107202 (2018).
[36] D. S. Rokhsar and S. A. Kivelson, Superconductivity and the Quantum Hard-Core Dimer Gas, Phys. Rev. Lett. **61**, 2376 (1988).
[37] R. Moessner and S. L. Sondhi, Resonating Valence Bond Phase in the Triangular Lattice Quantum Dimer Model, Phys. Rev. Lett. **86**, 1881 (2001).
[38] A. Y. Kitaev, Fault-tolerant quantum computation by anyons, Ann. Phys. (Amsterdam) **303**, 2 (2003).
[39] S. R. White, Density Matrix Formulation for Quantum Renormalization Groups, Phys. Rev. Lett. **69**, 2863 (1992).
[40] See Supplemental Material at http://link.aps.org/supplemental/10.1103/PhysRevLett.127.097002 for more details and results, which includes Refs. [41,42].
[41] P. Calabrese and J. Cardy, Entanglement entropy and quantum field theory, J. Stat. Mech. (2004) P06002.
[42] M. Fagotti and P. Calabrese, Universal parity effects in the entanglement entropy of XX chains with open boundary conditions, J. Stat. Mech. (2011) P01017.
[43] S. R. White, I. Affleck, and D. J. Scalapino, Friedel oscillations and charge density waves in chains and ladders, Phys. Rev. B **65**, 165122 (2002).
[44] H.-C. Jiang, Superconductivity in the doped quantum spin liquid on the triangular lattice, npj Quantum Mater. **6**, 71 (2021).
[45] Y.-F. Jiang and H.-C. Jiang, Topological Superconductivity in the Doped Chiral Spin Liquid on the Triangular Lattice, Phys. Rev. Lett. **125**, 157002 (2020).
[46] It is difficult to determine whether the likely SC state in 2D is fully gapped or has gapless nodal quasiparticles. The large value of ξ_G we find might be taken as evidence of a small finite-size gap in what would become a gapless spectrum in the 2D limit, but this is far from certain.
[47] H.-C. Jiang, T. Devereaux, and S. A. Kivelson, Holon Wigner Crystal in a Lightly Doped Kagome Quantum Spin Liquid, Phys. Rev. Lett. **119**, 067002 (2017).
[48] C. Peng, Y.-F. Jiang, D.-N. Sheng, and H.-C. Jiang, Doping quantum spin liquids on the kagome lattice, Adv. Quantum Technol. **4**, 2000126 (2021).
[49] C. Peng, Y.-F. Jiang, T. P. Devereaux, and H.-C. Jiang, Evidence of pair-density wave in doping Kitaev spin liquid on the honeycomb lattice, npj Quantum Mater. **6**, 64 (2021).
[50] H.-C. Jiang and S. A. Kivelson, Stripe order enhanced superconductivity in the hubbard model, arXiv:2105.07048.
[51] V. J. Emery and S. A. Kivelson, Importance of phase fluctuations in superconductors with small superfluid density, Nature (London) **374**, 434 (1995).
[52] S. Gong, W. Zhu, and D. N. Sheng, following Letter, Robust d-Wave Superconductivity in the Square-Lattice t-J Model, Phys. Rev. Lett. **127**, 097003 (2021).
[53] S. Jiang, D. J. Scalapino, and S. R. White, Ground state phase diagram of the t-t'-J model, arXiv:2104.10149.